J Neurophysiol
88: 1197–1211, 2002; 10.1152/jn.00032.2002.

Muscarinic Activation of a Cation Current and Associated Current Noise in Entorhinal-Cortex Layer-II Neurons

MARK H. SHALINSKY,[1] JACOPO MAGISTRETTI,[1,2] LI MA,[1] AND ANGEL A. ALONSO[1]
[1]*Department of Neurology and Neurosurgery, Montreal Neurological Institute, McGill University, Montreal, Quebec H3A 2B4, Canada; and* [2]*Dipartimento di Scienze Fisiologiche-Farmacologiche Cellulari-Molecolari, Sezione di Fisiologia Generale e Biofisica Cellulare, Università degli Studi di Pavia, 27100 Pavia, Italy*

Received 15 January 2002; accepted in final form 6 May 2002

Shalinsky, Mark H., Jacopo Magistretti, Li Ma, and Angel A. Alonso. Muscarinic activation of a cation current and associated current noise in entorhinal-cortex layer-II neurons. *J Neurophysiol* 88: 1197–1211, 2002; 10.1152/jn.00032.2002. The effects of muscarinic stimulation on the membrane potential and current of in situ rat entorhinal-cortex layer-II principal neurons were analyzed using the whole cell, patch-clamp technique. In current-clamp experiments, application of carbachol (CCh) induced a slowly developing, prolonged depolarization initially accompanied by a slight decrease or no significant change in input resistance. By contrast, in a later phase of the depolarization input resistance appeared consistently increased. To elucidate the ionic bases of these effects, voltage-clamp experiments were then carried out. In recordings performed in nearly physiological ionic conditions at the holding potential of −60 mV, CCh application promoted the slow development of an inward current deflection consistently associated with a prominent increase in current noise. Similarly to voltage responses to CCh, this inward-current induction was abolished by the muscarinic antagonist, atropine. Current-voltage relationships derived by applying ramp voltage protocols during the different phases of the CCh-induced inward-current deflection revealed the early induction of an inward current that manifested a linear current/voltage relationship in the subthreshold range and the longer-lasting block of an outward K^+ current. The latter current could be blocked by 1 mM extracellular Ba^{2+}, which allowed us to study the CCh-induced inward current (I_{CCh}) in isolation. The extrapolated reversal potential of the isolated I_{CCh} was ≈0 mV and was not modified by complete substitution of intrapipette K^+ with Cs^+. Moreover, the extrapolated I_{CCh} reversal shifted to approximately −20 mV on removal of 50% extracellular Na^+. These results are consistent with I_{CCh} being a nonspecific cation current. Finally, noise analysis of I_{CCh} returned an estimated conductance of the underlying channels of ~13.5 pS. We conclude that the depolarizing effect of muscarinic stimuli on entorhinal-cortex layer-II principal neurons depends on both the block of a K^+ conductance and the activation of a "noisy" nonspecific cation current. We suggest that the membrane current fluctuations brought about by I_{CCh} channel noise may facilitate the "theta" oscillatory dynamics of these neurons and enhance firing reliability and synchronization.

INTRODUCTION

It has long been established that the cholinergic system plays a fundamental role in cortical function. Enhanced cortical acetylcholine release leads to cortical activation characteristic of waking and rapid-eye-movement (REM) sleep (Casamenti et al. 1986; Celesia and Jasper 1966) and cholinergic mechanisms mediated through muscarinic receptors have been implicated in different modalities of cortical plasticity (Dykes 1997; Richardson and DeLong 1988; Shulz et al. 2000) and memory function (Hasselmo and Bower 1993; Y. Tang et al. 1997). It is well known that, in most cases, muscarinic-receptor activation leads to direct depolarization of cortical principal neurons via the block of K^+ conductances (Benardo and Prince 1982a; Charpak et al. 1990; Halliwell and Adams 1982; Krnjevic 1993; Madison et al. 1987; McCormick and Prince 1986), and that the associated increase in excitability can be further enhanced by a inhibitory effect on Ca^{2+}-dependent K^+ currents (Cole and Nicoll 1984). In addition, muscarinic depolarizing drive mediated by the activation of nonselective cationic conductances has also been shown in several cortical (Benson et al. 1988; Colino and Halliwell 1993; Guérineau et al. 1995; Haj-Dahmane and Andrade 1998; McQuiston and Madison 1999; Segal 1982) and subcortical (Egan and North 1985) neuronal populations. Furthermore, muscarinic actions can also have a variety of other effects on the functional properties of mammalian neurons, such as modulation of voltage-gated Ca^{2+} currents (Allen and Brown 1993; Higashida et al. 1990; Mathie et al. 1992; Toselli and Taglietti 1995; Wanke et al. 1994, 1987), regulation of glutamatergic responses and synaptic transmission (Harvey et al. 1993; Hasselmo and Schnell 1994; Marino et al. 1998; Markram and Segal 1992), and changes in spike backpropagation through modulatory actions on dendritic conductances (Tsubokawa and Ross 1997).

The entorhinal cortex (EC) in the parahippocampal region receives a profuse cholinergic innervation from the basal forebrain that terminates primarily in layers II and V (Alonso and Kohler 1984; Alonso and Amaral 1995). During active states, the cholinergic system deeply influences the operations of the entorhinal-hippocampal network as reflected by the cholinergic-dependent emergence of population activities such as the "theta" rhythm, which, in EC, is largely generated by the layer II cells (Alonso and García-Austt 1987a). These neurons funnel neocortical information into the hippocampus via the perforant path (Andersen et al. 1966; Schwartz and Coleman 1981). Clarifying the actions of the cholinergic systems on EC

Address for reprint requests: A. Alonso, Dept. of Neurology and Neurosurgery, Montreal Neurological Institute, McGill University, 3801 University St., Montréal, Québec H3A 2B4, Canada (E-mail: angel.alonso@mcgill.ca).

The costs of publication of this article were defrayed in part by the payment of page charges. The article must therefore be hereby marked "*advertisement*" in accordance with 18 U.S.C. Section 1734 solely to indicate this fact.

layer-II neurons is thus fundamental for understanding the function(s) of the entorhinal-hippocampal network that is involved, at least, in the encoding of explicit memories (Scoville and Milner 1957; Squire 1998).

In a previous current-clamp study, we showed that application of the cholinergic agonist carbachol (CCh) to EC layer-II neurons resulted in a slowly developing, prolonged depolarization that pharmacological analysis revealed to be mediated primarily (if not exclusively) by the M1 muscarinic receptor subtype (Klink and Alonso 1997b,c). This muscarinic depolarization did not appear to be accompanied by an increase in membrane input resistance and was proposed to be caused by the activation of a nonspecific cation conductance (Klink and Alonso 1997c). However, a detailed characterization of this muscarinic depolarizing action and its ionic bases and mechanisms of activation is still missing in this, as well as other, neuronal populations. In the present investigation, we further analyzed the ionic bases of the depolarization induced by muscarinic stimuli in EC layer-II principal neurons by applying the whole cell, patch-clamp technique to obtain current- and voltage-clamp recordings from the same neurons in rat EC slices.

METHODS

Slice preparation

Brain slices were prepared from male Long-Evans rats (100–250 g, i.e., 30–60 days old) as previously described (Alonso and Klink 1993; Magistretti and Alonso 1999). Briefly, animals were decapitated according to a procedure approved by the Animal Care Committee of the Montreal Neurological Institute and compliant with the Canadian laws on animal research, and the brain was rapidly removed from the cranium and placed in a cold (4°C) Ringer solution containing (in mM) 124 NaCl, 5 KCl, 1.25 NaH_2PO_4, 2 $CaCl_2$, 2 $MgSO_4$, 26 $NaHCO_3$, and 10 glucose (pH 7.4 by saturation with 95% O_2-5% CO_2). Horizontal slices of the retrohippocampal region were cut at 350–400 μm on a vibratome (series 1000, Pelco, Redding, CA), and then transferred to an incubation chamber in which they were kept submerged for $\geq$1 h period at room temperature (24°C) before starting the recording.

Patch-clamp, whole cell recordings

The recording chamber was mounted on the stage of an upright microscope (see following text). Slices were transferred, one at a time, to the chamber and perfused with one of the extracellular solutions described in Table 1, according to the specific experimental purpose. Patch pipettes were fabricated from thick-wall borosilicate glass capillaries by means of a Sutter P-97 horizontal puller. The solutions used to fill the patch pipettes are also described in Table 1. When filled with one of these solutions, the patch pipettes had a resistance of 3–5 MΩ. Slices were observed with an Axioskop microscope (Zeiss, Oberkochen, FRG) equipped with a $\times$40 water-immersion objective lens and differential-contrast optics. A near-infrared charge-coupled device (CCD) camera (Sony XC-75) was also connected to the microscope and used to improve cell visualization for identification of neuron types and during the approaching and patching procedures. With this equipment, the principal cells of EC layer II were easily distinguished based on their somato-dendritic shape, size, and position (Dickson et al. 2000; Klink and Alonso 1997a). Patch pipettes were brought in close proximity to the selected neurons while manually applying positive pressure inside the pipette. Tight seals (>10 GΩ) and the whole cell configuration were obtained by suction (Hamill et al. 1981). Series resistance (R_s), as estimated on-line by canceling the fast component of whole cell capacitive transients evoked by $-$10-mV voltage steps with the amplifier compensation section (with the low-pass filter set at 10 kHz), and reading out the corresponding value, was on average approximately 16–18 MΩ. R_s was always compensated by ~40% with the amplifier's built-in compensation section. Current- and voltage-clamp recordings were performed at room temperature (~24°C) using an Axopatch 1D amplifier (Axon Instruments, Foster City, CA). The low-pass filter ($-$3 dB) was set at 5 kHz. In voltage-clamp recordings, the general holding potential was $-$60 mV.

CCh application and chemicals

Muscarinic responses were evoked with CCh delivered to the recorded cells by either bath perfusion or local pressure application, always at a holding potential of $-$60 mV. In the case of local application, a Picospritzer II (General Valve, Fairfield, NJ) was employed. The outlet of the Picospritzer was connected, via a nylon-wall tubing and a teflon holder, to the inside of a patch pipette (diameter at the tip $\approx$5 μm) filled with an osmotically balanced solution containing 100 mM CCh. The tip of the CCh-containing pipette was posi-

TABLE 1. *Composition of extracellular recording and intrapipette solutions*

Extracellular Solutions	NaCl	NMDG	$NaHCO_3$	KCl	CsCl	$MgCl_2$	$CaCl_2$	$BaCl_2$	D-glucose
A_o	125	—	26	5	2	2	2	—	10
B_o	125	—	26	5	2	2	2	1	10
C_o	49.5	75.5	26	5	2	2	2	—	10
Intrapipette Solutions	**K^+ Gluconate**	**Cs^+MeS**	**KCl**	**CsCl**	**NaCl**	**$MgCl_2$**	**HEPES**	**EGTA**	**BAPTA**
A_i	125	—	5	—	5	2	10	10	—
B_i	130	—	5	—	5	2	10	0.5	—
C_i	—	115	—	5	5	2	10	—	10
D_i	—	130	—	5	5	2	10	0.5	—

Solutions employed in the patch-clamp experiments of the present study. All concentrations are indicated in mmol·l^{-1}. All extracellular solutions were also added with the synaptic blockers, kynurenic acid (1 mM) and picrotoxin (100 μM), the nicotinic-receptor antagonists, mecamylamine (10 μM) and α-bungarotoxin (100 nM), and 300 nM tetrodotoxin. The pH of extracellular solutions was maintained at 7.4 by continuous bubbling with 95% O_2-5% CO_2. All intracellular solutions were added with 2 mM adenosine 5′-triphosphate (ATP) and 0.4 mM guanosine 5′-triphosphate (GTP). The pH of intracellular solutions was adjusted at 7.2 with KOH (A_i and B_i) or CsOH (C_i and D_i). NMDG, *N*-methyl-D-glucamine; Cs^+ MeS, Cs^+ methanesulphonate; HEPES, *N*-[2-hydroxyethyl]piperazine-*N*′-[2-ethanesulphonic acid]; EGTA, ethylene glycol-bis (β-aminoethyl ether) *N,N,N*′,*N*′-tetraacetic acid; BAPTA, 1,2-bis(2-aminophenoxy)ethane-*N,N,N*′,*N*′-tetraacetic acid.

tioned, under microscopic control, just above the slice surface in close proximity to the recording electrode. Pressure application was triggered manually, and its duration was normally set at 7–15 s.

All chemicals and reagents, including those listed in Table 1 and CCh, were purchased from Sigma (St. Louis, MO) except tetrodotoxin, which was purchased from Alomone Labs (Jerusalem, Israel).

Data acquisition

All recordings were stored on VHS tape by PCL coding using a Neurocorder converter (Neurodata, New York, NY). In voltage-clamp experiments, voltage protocols were commanded and current signals were acquired with a Pentium PC interfaced to an Axon DigiData 1200 interface, using the Clampex program of the pClamp software (V8.0, Axon Instruments). Ramp voltage protocols consisted of 30- or 10-s linear depolarizations from −100 to −40 or −30 mV, always preceded by a 2-s fixed step at −100 mV. Data stored on VHS tape was digitized and plotted off-line by sampling at 10 kHz using the AxoScope or software (Axon Instruments).

Data analysis

Whole cell recordings were analyzed by means of the Clampfit program of the pClamp software (Axon Instruments). Linear regressions as well as fittings with nonlinear functions were performed using Origin 6.0 (MicroCal Software, Northampton, MA). Linear fitting for the estimation of the reversal potential of the CCh-induced cation current was always done for the voltage range of −100 to −60 mV. High-pass filtering of current traces and variance calculations were conducted using Clampfit or Origin.

For variance analysis, current traces recorded during CCh responses were partitioned into 500-ms consecutive segments, over each of which average current amplitude (I_{mean}) and current variance (σ_I^2) values were calculated. σ_I^2 values were then plotted as a function of I_{mean}, and the resulting plots were fitted with the theoretical parabolic function (Sigworth 1980)

$$\sigma_I^2 = i \cdot I_{mean} - I_{mean}^2/N + \sigma_{I\,base}^2 \quad (1)$$

where i is the single-channel current amplitude, N is the total number of channels, and $\sigma_{I\,base}^2$ is the current variance due to background noise. The preceding equation holds under the assumption that the current under study is generated by a functionally homogeneous population of channels in which the probability of observing a given number of channels open at any time point can be described according to a binomial distribution (Anderson and Stevens 1973; Hille 1992).

For spectral analysis, two 4-s trace stretches corresponding to baseline and peak I_{CCh} response, each of which could be considered as stationary with respect to average current level over time, were selected for each of the CCh responses analyzed. Spectral (Fourier) analysis of current fluctuations was carried out using Clampfit. Binned power density values relevant to baseline were subtracted from those derived from the CCh response, and a power density spectrum was then constructed for each cell analyzed. Power spectra were fitted with single Lorentzian functions in the form

$$S(f) = S_0/[1 + (f/f_c)^2] \quad (2)$$

where f is frequency, and f_c, the corner frequency of the function, equals $(1/\tau_o + 1/\tau_c)/2\pi$, τ_o and τ_c being the channel mean open and closed times, respectively. Under the assumption of a low channel-opening probability, the quantity $\tau = 1/2\pi f_c$ thus provides an approximation to τ_o.

Average values were expressed as means ± SE. Statistical significance was evaluated by means of the two-tail Student's *t*-test for unpaired data.

RESULTS

Muscarinic stimulation induces prolonged depolarizations associated with composite effects on membrane resistance

Current-clamp experiments on the voltage responses induced by muscarinic stimulation in EC principal neurons were first carried out. In these recordings, tetrodotoxin (TTX; 1 μM) and Cs^+ (2–4 mM) were added to the extracellular solution to block voltage events dependent, respectively, on voltage-gated Na^+ currents and the hyperpolarization-activated cation current, I_h (Dickson et al. 2000). The extra- and intracellular solutions used were solutions A_o and A_i, respectively (see Table 1). Under these conditions, bath application of CCh (30–100 μM) resulted in the development of a slow, long-lasting depolarization, as in the case illustrated in Fig. 1*A*. This depolarization could be above-threshold for the elicitation of transient regenerative potentials, probably Ca^{2+} spikes (Fig. 1*A*, arrows). No detectable depolarization was evoked by CCh in the presence of the muscarinic antagonist, atropine (1 μM; $n = 3$). The initial, rising phase of CCh-dependent depolarization (Fig. 1*B*) was accompanied by either a slight decrease or no significant change in input resistance as monitored by measuring the amplitude of the voltage deflections induced by repetitively applied small hyperpolarizing current pulses (Fig. 1*D*). By contrast, during later phases of CCh-induced depolarization (Fig. 1*C*) a sustained increase in input resistance was consistently observed (Fig. 1*D*). Very similar results were obtained from nine other neurons. These findings prompted the working hypothesis that the depolarization evoked by muscarinic stimulation in the neurons under study depends on both the activation of a conductance responsible for an inward current, and the block of a conductance responsible for an outward current, the latter effect being more persistent than the former and prevalent during late phases.

Muscarinic stimulation causes transient activation of an inward current and persistent block of an outward K^+ current

To directly clarify the nature of the ionic conductance(s) implied in the depolarizing action of CCh, voltage-clamp experiments were then undertaken. We first tested the effects of bath-applied CCh (30–100 μM for 30–120 s) using an intrapipette solution containing K^+ (gluconate salt) as the main cation, as well as 10 mM EGTA to provide a relatively high intracellular Ca^{2+}-buffering capacity (intracellular solution A_i). The extracellular recording solution (solution A_o) was always added with 1 μM TTX and 2–4 mM Cs^+ (see preceding text) as well as mecamylamine (10 μM) and α-bungarotoxin (100 nM) to block possible nicotinic responses arising on CCh application. As in the case illustrated in Fig. 2, cells were always held at −60 mV and, to explore current-voltage (*I-V*) relationships, slow voltage-ramp protocols (see METHODS) were applied prior to CCh, at the peak of the CCh response, and during recovery (*A*). In all neurons tested in this manner ($n = 8$), CCh always induced an inward current that, after reaching a peak in 122.5 ± 27.6 s, slowly decayed toward the baseline during washout. The peak amplitude of this inward current deflection averaged −114.3 ± 19.9 pA. Bath application of CCh in the presence of atropine (1 μM; $n = 4$) or the M1 antagonist pirenzipine (1 μM; $n = 4$) never resulted in any significant change in holding current.

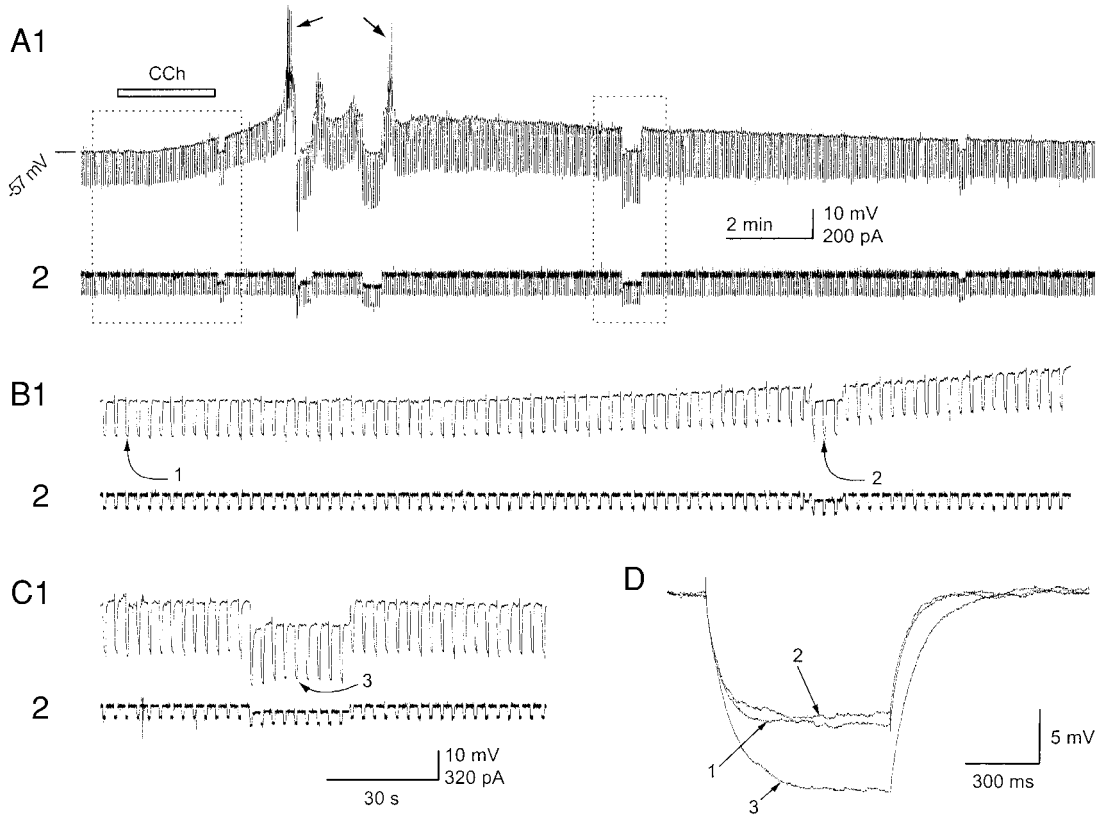

FIG. 1. Effects of carbachol (CCh) stimulation on membrane potential and input resistance of entorhinal cortex (EC) layer-II principal neurons. *A*: current-clamp recording in a representative neuron (*cell 9732000*). The recording solutions used were solutions A_o and A_i (see Table 1). *A*, *1* and *2*, illustrates the voltage recording and the current command, respectively. During and after the application of CCh (40 μM) by bath superfusion (horizontal bar), a slow membrane depolarization was produced. The depolarization eventually reached the threshold for the generation of Ca^{2+} spikes (arrows) that were terminated by negative steady-current injection (*A2*). *B* and *C*: the trace stretches delimited by the left (for *B*) and right (for *C*) boxes in *A* are shown over an expanded time scale (here again, *1* and *2* illustrate the voltage recording and the current command, respectively). Note the negative current square pulses (*B2* and *C2*) repetitively delivered to monitor the input resistance. *D*: the current deflections elicited by 3 identical hyperpolarizing current steps during 3 different phases of the recording: control conditions (1: see *B1*), early CCh-dependent depolarization (2: see *B1*), late CCh-dependent depolarization (3: see *C1*).

As shown in *B*, at the peak of the current response induced by CCh the *I-V* relationship always displayed an inward shift with respect to the control *I-V* over the entire voltage range explored (-100 to $-40/-30$ mV). This indicates that, at its maximum, the CCh-induced current inward deflection cannot be primarily attributed to the block of a K^+ conductance but rather arises from the activation of an inward current. Indeed, note (*A*) that the development of the CCh response was also associated with an evident increase in current noise indicative of the opening of previously silent ion channels during the response (this aspect will be treated in detail in the following text; see Fig. 6).

In addition, however, we also noticed that, despite the transient nature of the current response to CCh, the control current level was never fully recovered on washout (see Fig. 2*A*), even after waiting for tens of minutes. Rather an apparent, residual "background" inward current remained persistently induced (*). The inward current deflection persisting after 20 min from the peak averaged 14.5 $\pm$ 2.4 pA ($n = 5$), namely ~12.7% of the peak amplitude. Moreover in contrast with *I-V* protocols applied at the peak of the CCh response, washout *I-V*s did display a decrease in slope conductance with respect to control *I-V*s (Fig. 2*B*). These observations indicate that the response to CCh observed at -60 mV is actually the result of a mixed action that includes, in addition to the transient activation of an inward current, the long-lasting block of an outward current, presumably carried by K^+.

Consistent with the idea that CCh persistently blocks a K^+ conductance, the current obtained by subtracting the washout *I-V* from the control *I-V* (Fig. 2, *B* and *D*) reversed at -76.4 ± 2.6 mV ($n = 6$) in control Ringer solution (extracellular K^+ concentration, $[K^+]_o$, = 5 mM). Even more importantly, in recordings performed in the presence of 10 mM extracellular K^+ the same current reversed at -60.3 ± 2.6 mV ($n = 3$). This represents a positive shift of about +16 mV, a value in close agreement with what theoretically predicted on the basis of the Nernst equation for a twofold increase in $[K^+]_o$ (+17.7 mV).

We took advantage of the rather persistent character of the K^+-conductance block in response to a first application of CCh in a first attempt to extract the real inward current resulting from CCh-induced activation of ion conductance(s) and to examine, during a second CCh application, its *I-V* relationship in relative isolation. Note in Fig. 2*C* that, in the case of a second CCh application, control (trace 3; washout from the 1st application) and washout (trace 4) *I-V*s did display a good overlap, thus suggesting that second applications did not cause any further K^+-conductance block. Subtraction of the control *I-V* from the CCh *I-V* (Fig. 2*E*) revealed that the CCh-activated

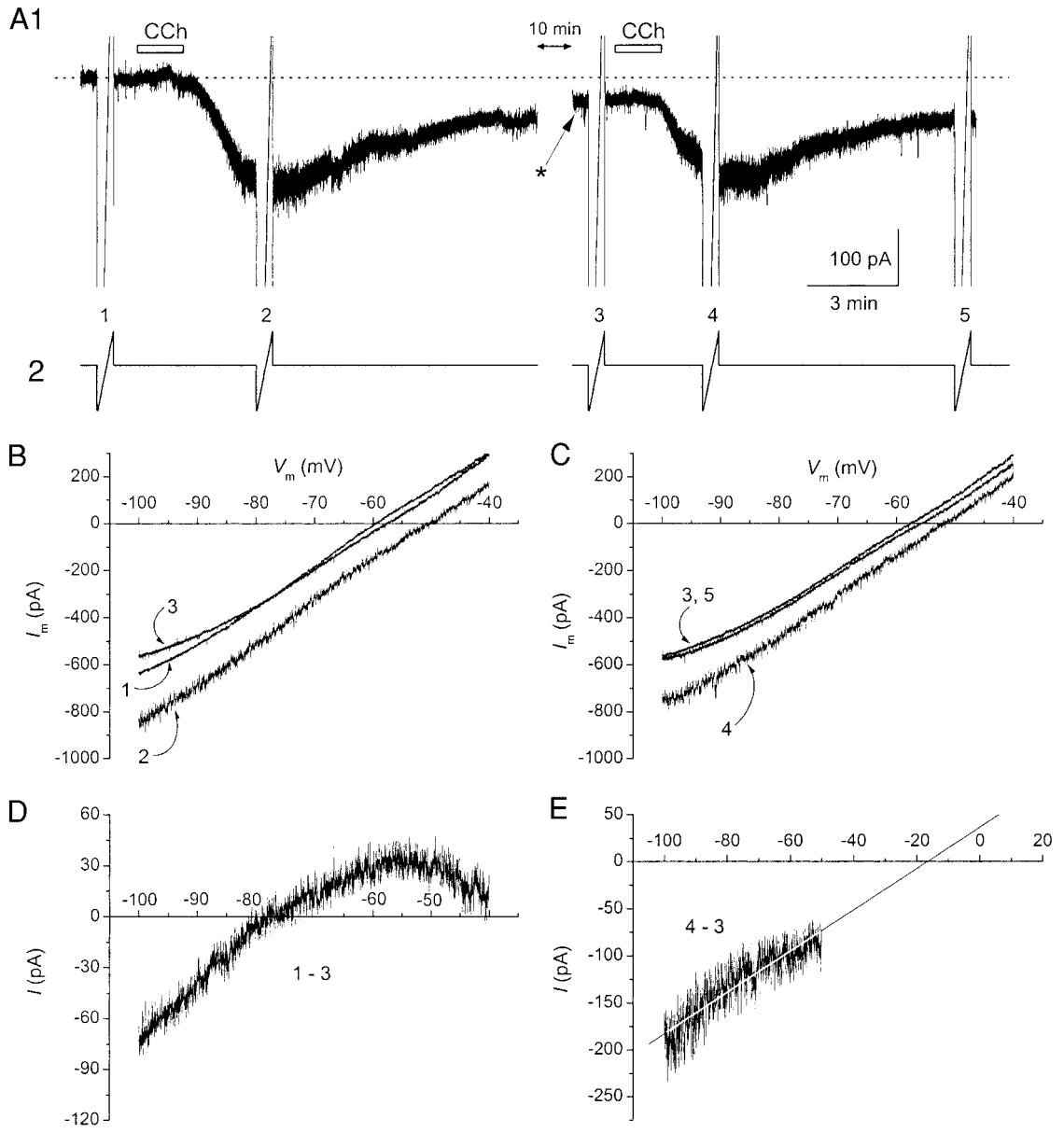

FIG. 2. Depolarizing current response to CCh stimulation comprises activation and block of 2 different current components. *A*: voltage-clamp recording in a representative neuron (*cell 98010502*) in the presence of K^+ as the main intracellular cation and 10 mM intrapipette EGTA (recording solutions: A_o and A_i). CCh was delivered by bath superfusion during the periods marked (□). The 2nd CCh application started ~23 min after the 1st one. Before and during the CCh responses, slow depolarizing voltage ramps (see METHODS) were commanded (*A2*). Note that, after the 1st CCh application, a sustained inward current deflection remained persistently induced (*) even after as long as ~22 min of washout. *B* and *C*: the currents recorded in response to ramp protocols 1–5 of *A*, plotted as a function of ramp voltage. Note in *B* that, after CCh washout, a current component that was outward at −60 mV was inhibited with respect to control conditions, thus causing a decrease in the slope conductance of the *I-V* plot (compare 1 and 3). *D*: the *I-V* relationship of the current obtained by subtracting ramp current 1 (control) from ramp current 3 (washout). Current reversal was at about −77 mV. *E*: the *I-V* relationship of the current obtained by subtracting ramp current 4 (CCh, 2nd application) from ramp current 3 (washout from the 1st application). The straight line is the linear regression to data points, which returned an extrapolated reversal potential of −16.3 mV.

inward current decreased linearly with voltage in the range from −100 to about −60/−50 mV and displayed an extrapolated reversal potential of −16.8 mV; this is consistent with this current being mediated by a nonspecific cation conductance (see following text). Similar results were obtained in the two other cells in which the same protocol was applied.

In further experiments, 1 mM Ba^{2+}, a cation known to block leak and inward rectifying K^+ conductances, was added to the recording solution (extracellular solution B_o) in the attempt to exclude the K^+ conductance(s) negatively modulated by CCh and thereby isolate the CCh-induced inward current presumably resulting from the activation of a nonspecific cation conductance. As in the case shown in Fig. 3*A*, application of CCh in the presence of extracellular Ba^{2+} always resulted in the induction of an inward current that washed out almost completely. In these conditions, the inward current peak amplitude averaged −71.4 ± 15.7 pA (n = 5), whereas the current persisting at approximately 15 min after the peak averaged

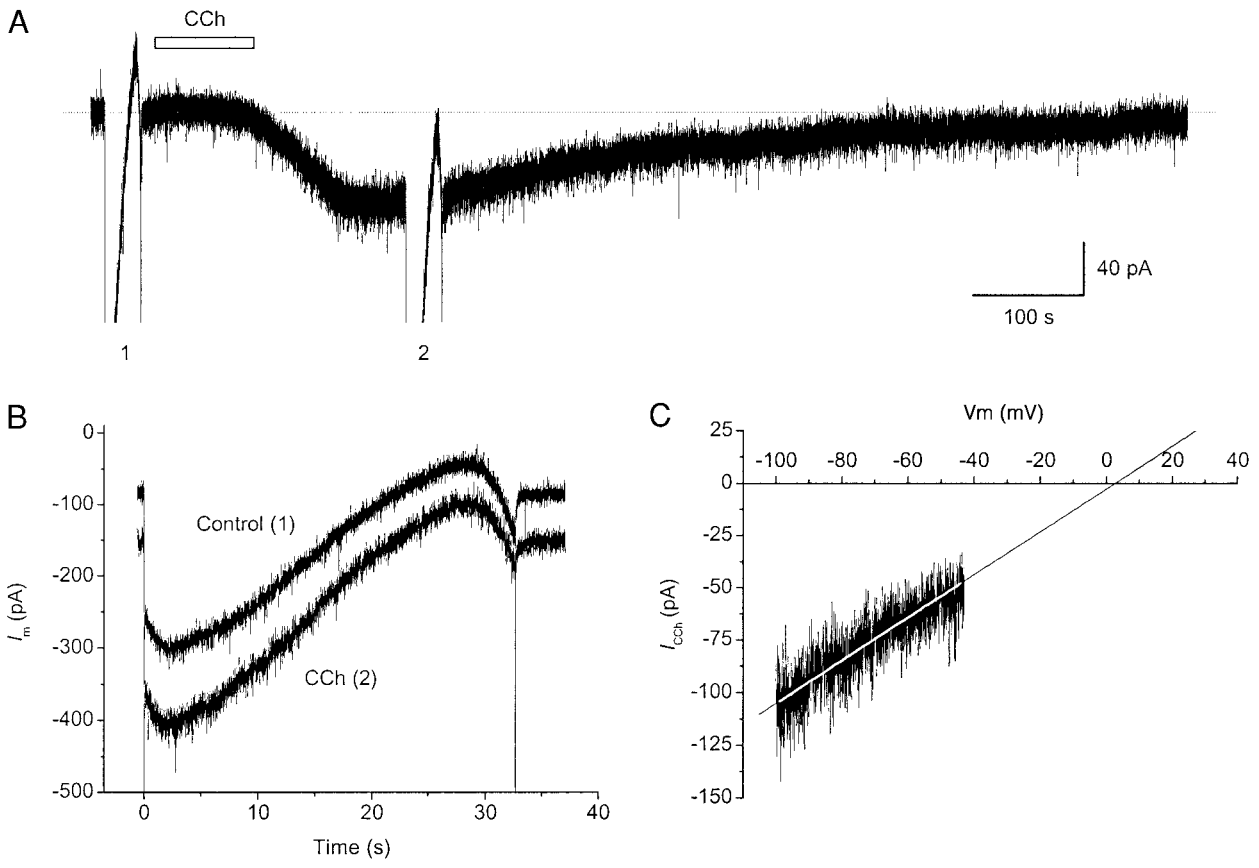

FIG. 3. CCh activates an inward current in isolation in the presence of 1 mM extracellular Ba^{2+}. *A*: current response to CCh application in a representative neuron (*cell 97121704*) recorded in intracellular K^+ and 10 mM EGTA (intracellular solution A_i) and in the presence of 1 mM Ba^{2+} in the extracellular solution (extracellular solution B_o). CCh was delivered by bath superfusion (□). Note the 2 ramp protocols (1 and 2) commanded before and during the CCh response. *B*: the currents recorded in response to ramp protocols 1 (control) and 2 (CCh) of *A*, plotted as a function of time. *C*: the *I-V* relationship of the CCh-induced current (I_{CCh}), obtained by subtracting ramp current 1 from ramp current 2. —, the linear regression to data points, which returned an extrapolated reversal potential of +2.8 mV.

-3.7 ± 2.3 pA, namely $5.8 \pm 3.8\%$ of the peak ($n = 5$). The *I-V* relationship under CCh displayed the typical inward shift with respect to the control *I-V* (*B*), and the CCh-induced inward current obtained by subtraction always decreased linearly with voltage in the range between −100 and about −60 mV (*C*). Application of voltage ramps after CCh-induced-current washout revealed no sign of further decrease in slope conductance nor of sustained block of an outward (K^+) current (not shown). Because 1 mM extracellular Ba^{2+} proved efficient in blocking CCh-inhibited K^+ current, thereby isolating the inward current activated by CCh, this cation was always used at the same concentration in all of the experiments conducted in intracellular K^+ described from this point on.

CCh-activated inward current is a nonspecific cation current

The ionic nature of the inward current activated by CCh (I_{CCh}) was further investigated by analyzing its reversal potential in recordings carried out with K^+ as the main intracellular cation. These experiments were performed in the presence of either 10 mM EGTA (such as those illustrated so far; $n = 3$) or 0.5 mM EGTA ($n = 5$) in the intrapipette solution (intracellular solutions A_i and B_i) because the *I-V* relationship of I_{CCh}, as examined by means of slow depolarizing ramps and isolated by subtraction, behaved very similarly in the two conditions. The current's reversal potential, derived by extrapolating to $I = 0$ the linear fitting of the *I-V* relationship in its negative voltage range (about −100/−60 mV) and estimated by pooling the high- and low-EGTA data together, averaged $+0.2 \pm 4.5$ mV ($n = 8$). As mentioned in the preceding text, this estimated reversal potential is consistent with I_{CCh} being mediated by a nonspecific cation conductance. The estimation of the reversal potential was made, however, on the assumption that the slope conductance remained constant over the voltage range of extrapolation.

We then examined the effects on I_{CCh} of substituting K^+ with Cs^+ (methanesulphonate salt) as the main intracellular cation (intracellular solution C_i or D_i). Due to the efficient blocking action of intracellular Cs^+ on K^+ conductances, in these experiments, Ba^{2+} was omitted from the extracellular recording solution (extracellular solution A_o). Similarly to what observed in the presence of intracellular K^+, in all cells tested in these conditions ($n = 23$), CCh applications resulted in the development of a slow inward current accompanied by an evident increase in membrane current noise (see Fig. 4*A*). The *I-V* relation of the CCh-induced inward current was also derived from slow depolarizing ramp protocols, by means of the usual subtraction procedure. Here again, current amplitude was found to always decay linearly with increasingly positive volt-

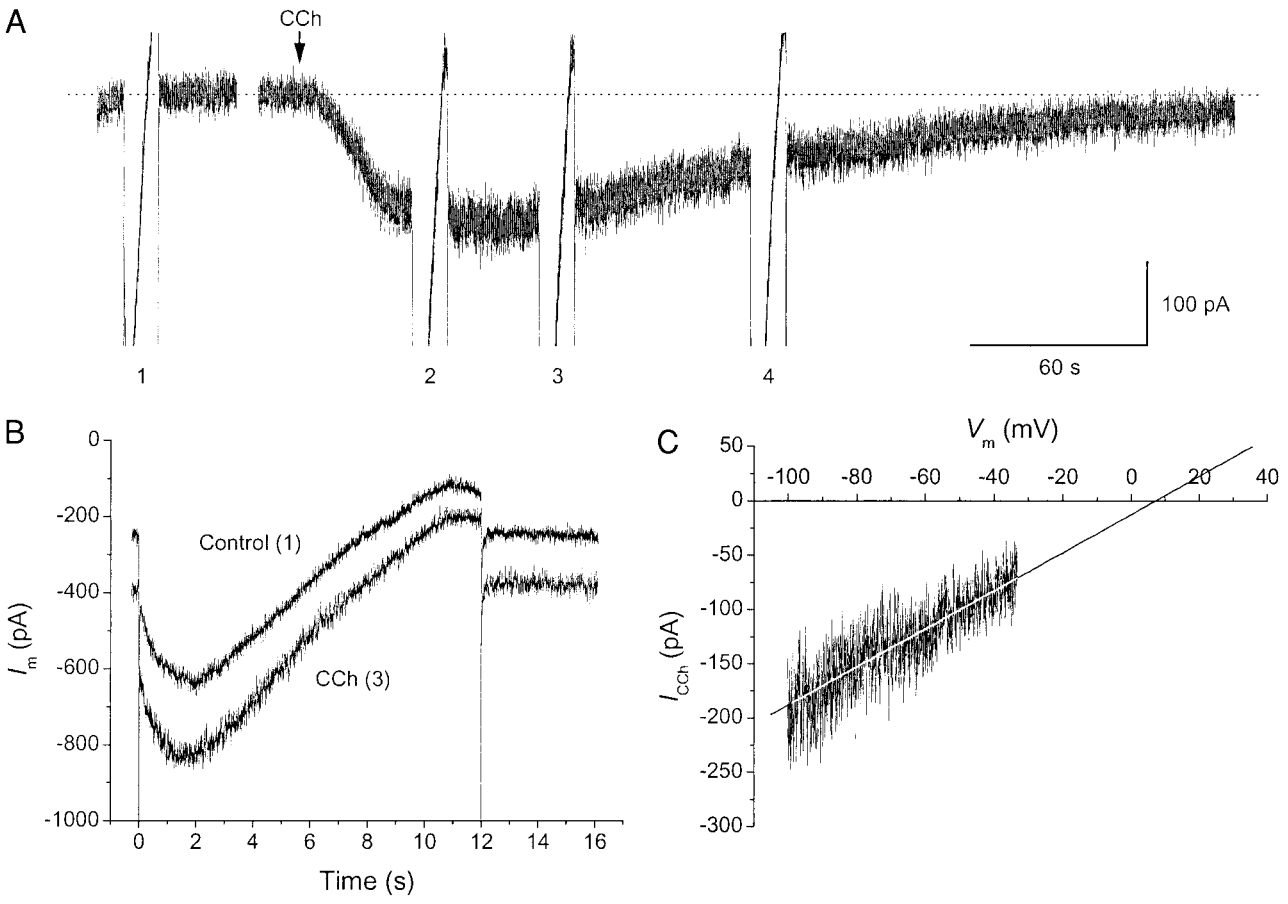

FIG. 4. CCh-induced current in the presence of Cs^+ as the main intracellular cation. *A*: current response to CCh application in a representative neuron (*cell 0051102*) recorded in intracellular Cs^+ and 10 mM BAPTA (recording solutions: A_o and C_i). CCh was delivered by pressure application (14 s), starting from the time point marked by the ↓. Note the 4 ramp protocols (1–4) commanded before and during the CCh response. A 120-s baseline segment between ramp 1 and CCh application has been omitted. *B*: the currents recorded in response to ramp protocols 1 (control) and 3 (CCh) of *A*, plotted as a function of time. *C*: the *I-V* relationship of the CCh-induced current (I_{CCh}), obtained by subtracting ramp current 1 from ramp current 3. —, the linear regression to data points, which returned an extrapolated reversal potential of +7.2 mV.

ages in a range between −100 and about −50 mV (Fig. 4*B*). Linear fittings returned an average extrapolated reversal potential of −0.1 ± 3.1 mV (n = 15), a value not significantly different from that observed in neurons recorded with K^+ as the main intracellular cation. These data further indicate that I_{CCh} is mediated by a nonspecific cation conductance and suggest that it has similar permeabilities for K^+ and Cs^+. Therefore from this point on, we will refer to this non-specific cation current dependent on muscarinic-receptor activation as I_{NCM}.

To determine whether under normal extracellular ionic conditions, a substantial part of the inward I_{NCM} is carried by Na^+, we performed experiments in which half of the extracellular Na^+ was substituted with equimolar *N*-methyl-D-glucamine (extracellular solution C_o) in the presence of Cs^+ as the main intracellular cation (intracellular solution C_i or D_i). Application of CCh in these conditions (Fig. 5) evoked an inward current whose extrapolated reversal potential averaged −21.0 ± 2.5 mV (n = 7). This represents a reversal shift, with respect to recordings carried out in normal extracellular Na^+, of −21.1 mV thus confirming that I_{NCM} is substantially carried by Na^+.

Fluctuation analysis of I_{NCM}

We then approached the identification of the channels mediating I_{NCM} by taking advantage of the prominent increase in current noise associated with I_{NCM} activation (see for instance Figs. 2–4). In 11 neurons recorded with intrapipette Cs^+ methanesulphonate, current recordings were performed at a high gain, filtered at 5 kHz, and digitized at 10 kHz. The extracellular recording solution also contained glutamatergic and GABAergic antagonists (see Table 1, legend) to avoid potential contamination by miniature synaptic events. High-pass filtering of individual CCh responses eliminated the DC component as well as the slow current deflections and revealed an increase in high-frequency current fluctuations that closely followed the slow time course of the responses (Fig. 6*A*, *top trace*). This increase in current noise reflects the stochastic gating of the underlying channels (Hille 1992). To evaluate the unitary properties of these channels, we applied the methods of fluctuation analysis (Anderson and Stevens 1973) to I_{NCM} responses. For this purpose, I_{NCM} traces were partitioned into 500-ms intervals, during which the changes in mean current level over time were negligible (Fig. 6*A*, *bottom expanded traces*), and in each trace segment thus obtained current vari-

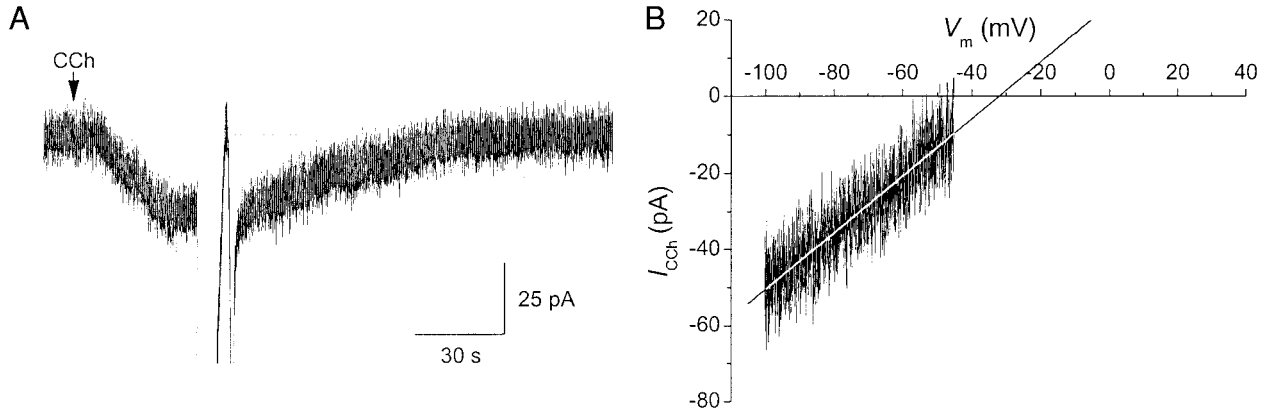

FIG. 5. CCh-induced current after removal of 50% extracellular Na^+. *A*: current response to CCh application in a representative neuron (*cell 0062001*) recorded in intracellular Cs^+ and 10 mM bis-(o-aminophenoxy)-*N*,*N*,*N*′,N′-tetraacetic acid (BAPTA, intracellular solution C_i), and after substitution of 50% extracellular Na^+ with equimolar *N*-methyl-D-glucamine (NMDG, extracellular solution C_o). CCh was delivered by pressure application (15 s). Note the ramp protocol commanded at the peak of the CCh response. *B*: the *I-V* relationship of the CCh-induced current (I_{CCh}), obtained by ramp-current subtraction. The straight line is the linear regression to data points, which returned an extrapolated reversal potential of −31.9 mV.

ance (σ_I^2) and mean current amplitude (I_{mean}) were measured. Plots of σ_I^2 as a function of I_{mean} were then constructed (Fig. 6*B*). Assuming that the macroscopic current is generated by the superimposition of identical, independent channel openings that have a single conductive state, the relationship between σ_I^2 and I_{mean} can be described by the parabolic function given by *Eq. 1* (see METHODS). Note in the exemplary case illustrated in Fig. 6 how the $\sigma_I^2(I_{mean})$ plot was basically linear for small

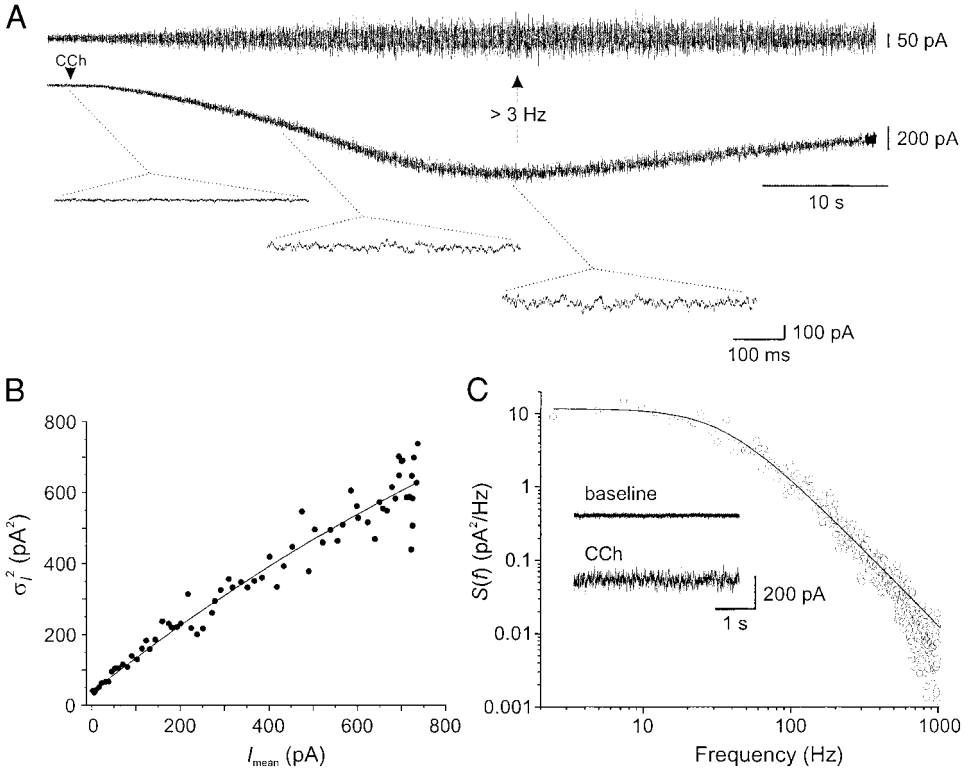

FIG. 6. Fluctuation analysis of CCh-induced current. *A*: current response to CCh application in a representative neuron (*cell 0050904*) recorded in intracellular Cs^+ (recording solutions: A_o and D_i). CCh was delivered by pressure application (10 s), and no voltage protocols were commanded during the CCh response. *Bottom*: the original current response; *top*: the same current low-pass filtered at 3 Hz to highlight the increase in high-frequency current noise associated with I_{CCh} activation. Three exemplary 500-ms segments of the original current trace, corresponding to control conditions, I_{CCh} onset, and I_{CCh} peak, are also shown over an expanded time scale in the *bottom part* of the panel. *B*: plot of current variance (σ_I^2) as a function of mean current amplitude (I_{mean}) for the I_{CCh} response shown in *A*. Every pair of σ_I^2 and I_{mean} values was derived from 500-ms trace stretches, such as those shown in the *A*, *bottom*, into which the original current recording was partitioned. —, the best parabolic fitting to data points, conducted on the basis of *Eq. 1* (see text). Fitting parameters were $i = 0.98$ pA, $n = 3996$, and $\sigma_{I\,base}^2 = 37.8$ pA^2. *C*: power density spectrum of I_{CCh} fluctuations, derived from the CCh response shown in *A*. The Fourier analysis was conducted on the 2 5-s current segments (baseline and CCh) shown in the *inset* (see the METHODS for details). The continuous line is the best fitting to data points obtained using a single Lorentzian function (*Eq. 2*), which returned a corner frequency of 34.6 Hz.

I_{NCM} amplitudes but then deviated from linearity as current amplitude approached its maximum value. Fitting the plot of Fig. 6*B* with *Eq. 1* yielded an estimate of *i* of 0.98 pA and an *N* of 3996. A satisfactory parabolic fitting was obtained in most ($n = 9$) cells analyzed. On average, the single-channel current amplitude at the holding potential of −60 mV was 0.81 ± 0.13 pA, which, given an average I_{NCM} reversal potential of −0.1 mV (see preceding text), corresponds to a single-channel conductance of 13.5 pS.

The temporal characteristics of the I_{NCM} channel openings were also examined by spectral density analysis of I_{NCM} current fluctuations (Anderson and Stevens 1973). The power density spectrum derived from the recording illustrated in Fig. 6*A* is depicted in *D*. Fitting of data points with a single Lorentzian function (*Eq. 2*) returned a corner frequency of 34.6 Hz, corresponding, under the assumption of a low channel-opening probability (see METHODS), to a mean open time (τ_o) of 4.69 ms. In nine neurons, the average, estimated channel τ_o was 6.63 ± 1.11 ms.

Lack of dependence of basal I_{NCM} induction on $[Ca^{2+}]_i$

As already mentioned, CCh responses could always be induced with an intracellular solution containing a high concentration (10 mM) of the Ca^{2+}-chelating agent, EGTA, thus suggesting that the induction of I_{NCM} may not be dependent on a rise in intracellular Ca^{2+} concentration ($[Ca^{2+}]_i$). To further test this possibility, we also performed experiments using a Cs^+-based intracellular solution containing 10 mM bis-(*o*-aminophenoxy)-*N*,*N*,*N*′,*N*′-tetraacetic acid (BAPTA), a Ca^{2+}-chelating agent known to be kinetically faster than EGTA in the Ca^{2+}-binding reaction (intracellular solution C_i). In these recordings conditions, CCh still triggered the activation of prominent I_{NCM}s in all neurons tested ($n = 7$; not shown). Indeed, the I_{NCM} peak amplitude observed in 10 mM intracellular BAPTA was −172.4 ± 79.4 pA ($n = 7$), a value not significantly different ($P > 0.4$) from that obtained in neurons recorded using a similar Cs^+-based pipette solution containing a low concentration (0.5 mM) of EGTA (intracellular solution D_i; −105.2 ± 43.3 pA; $n = 16$). This comparison was limited to recordings in which CCh was delivered by local pressure application under standard conditions (see METHODS). The lack of significant effects on I_{NCM} amplitude of the those illustrated in the preceding text increase in intracellular Ca^{2+}-binding capacity and efficacy favors the idea that I_{NCM} activation by muscarinic stimulation may not depend on $[Ca^{2+}]_i$ elevations under basal conditions.

$[Ca^{2+}]_i$-dependent modulation of CCh-induced inward-current responses

Although no significant difference in basal I_{NCM} amplitude was seen in the presence of high versus low $[Ca^{2+}]_i$-buffering capacity, different behaviors of the CCh-evoked responses were actually observed in the two conditions after the application of depolarizing ramps. When using 0.5 mM intrapipette

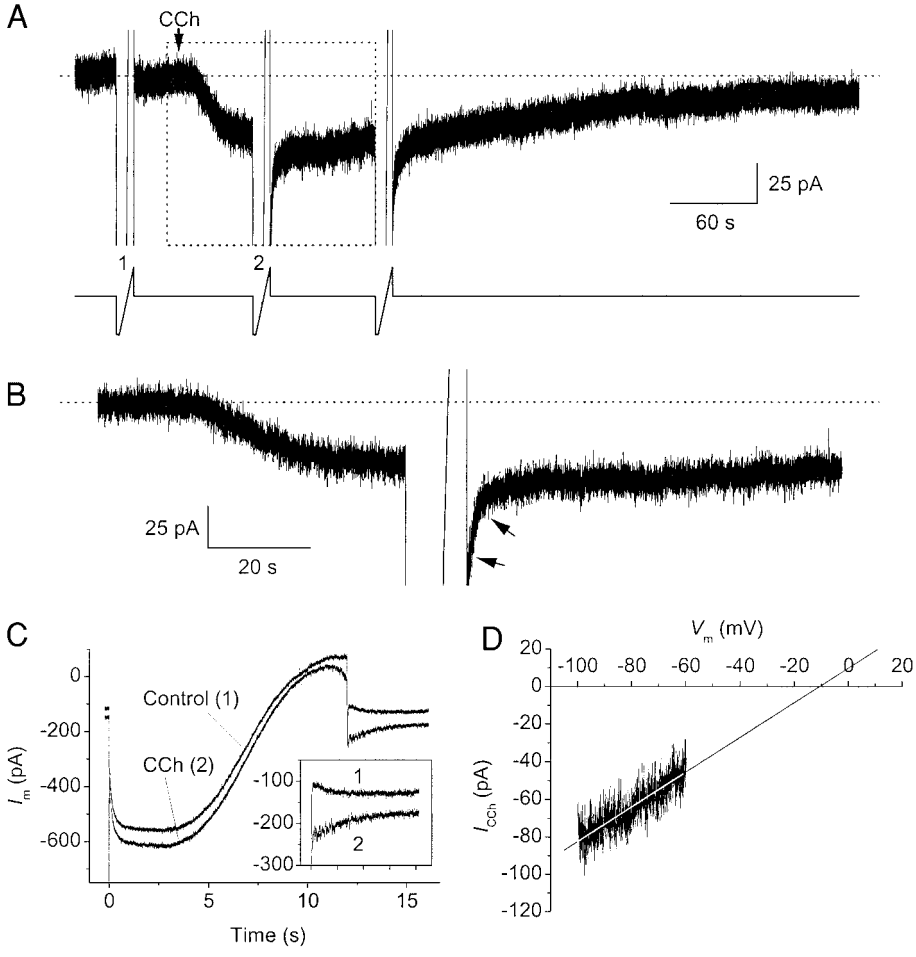

FIG. 7. Postramp potentiation of CCh-induced inward current in intracellular K^+. *A*: voltage-clamp recording in a representative neuron (*cell 0041103*) in the presence of 0.5 mM intra-pipette EGTA (recording solutions: A_i and A_o). CCh was delivered by pressure application (10 s), starting from the time point marked by the arrow. The *top* and *bottom traces* represent the current recording and the voltage command, respectively. Note the slow depolarizing voltage ramps (see METHODS) commanded before and during the CCh response. *B*: the trace delimited stretch (···) in *A* is shown over an expanded time scale. Note the postramp, "tail-like" transient increase in inward current (←). *C*: the currents recorded in response to the ramp protocols labeled 1 and 2 in *A*. *Inset*: a detail of the current traces after the end of the ramp depolarization (every division of the *x* axis is 1 s). - - -, the amplitude level of the CCh-induced current prior to ramp 2 application. *D*: the current obtained by subtracting control ramp current from CCh ramp current (currents 1 and 2 in *C*, respectively) as a function of ramp voltage. The straight line is the linear regression to data points, which returned an extrapolated reversal potential of −11.4 mV.

EGTA, but not 10 mM EGTA or BAPTA, the depolarizing ramp protocols applied during the CCh response were always followed by the immediate development of prominent, transient extra inward currents that turned off in some seconds (Fig. 7, *B*, ←, and 7*C*, *inset*) and had therefore the appearance of slowly decaying tail currents. On average, the maximal amplitude (I_{peak}) of these postramp currents (measured after subtracting the current baseline) was 2.60 ± 0.47 times that of the preramp current level (I_{pre}), and the half time of their decay, measured as the time interval between I_{peak} and a current level equal to (I_{pre} + I_{peak})/2, was 4.9 ± 1.4 s (n = 8). The slow, tail-like currents were also accompanied by an evident increase in current noise indicative of an increased channel activity (see Fig. 7*C*, *inset*). The appearance of these postramp, slow "tails" was strictly dependent on muscarinic stimulation because no similar currents developed following depolarizing ramp protocols in the absence of CCh application (see Fig. 7*A*).

Moreover, in the presence of Cs^+ (methanesulphonate salt), but not K^+, as the main intracellular cation, and 0.5 mM EGTA, ramp-triggered tail-like currents were always followed by a quick fall of I_{NCM} amplitude to levels marked lower to the preramp ones. The cell illustrated in Fig. 8, *A–D*, provides a typical example of the ramp-triggered sequence comprising tail-like-current induction and I_{NCM} downregulation. A voltage ramp applied at the peak of the CCh response was followed by an inward tail-like current (Fig. 8*C*) that decayed back to the preramp current level (- - -) in ~3–15 s. Additionally, however, this decay phase continued in a further, profound, relatively brisk decrease of the current level as compared with the preramp I_{NCM} amplitude (- - - in *A* and *B*). This I_{NCM} downregulation was accompanied by a marked reduction of current noise (Fig. 8*B*, *bottom*), indicative of a decrease of the underlying channel activity. Additional ramp protocols applied after the I_{NCM} downregulation caused by the first ramp resulted in further degrees of I_{NCM} decrease, up to basically the control (pre-CCh) level (Fig. 8*A*). Results very similar to those described for this neuron were obtained in eight other cells.

The preceding findings show that prominent changes in muscarinic-receptor-dependent inward-current induction can be caused by depolarizing stimuli provided $[Ca^{2+}]_i$ is not potently buffered to nearly zero. This strongly suggests that both phenomena (tail-like current elicitation and I_{NCM} downregulation) observed in the presence of 0.5 mM EGTA intracellular after the application of depolarizing ramps, depend on transient increases in $[Ca^{2+}]_i$ due to the voltage-dependent Ca^{2+} entry elicited by the depolarization itself. Hence, whereas $[Ca^{2+}]_i$ is not a primary factor in the mechanisms underlying basal I_{NCM} activation, it does appear to have a role in modulating muscarinic-receptor-dependent depolarizing current(s)

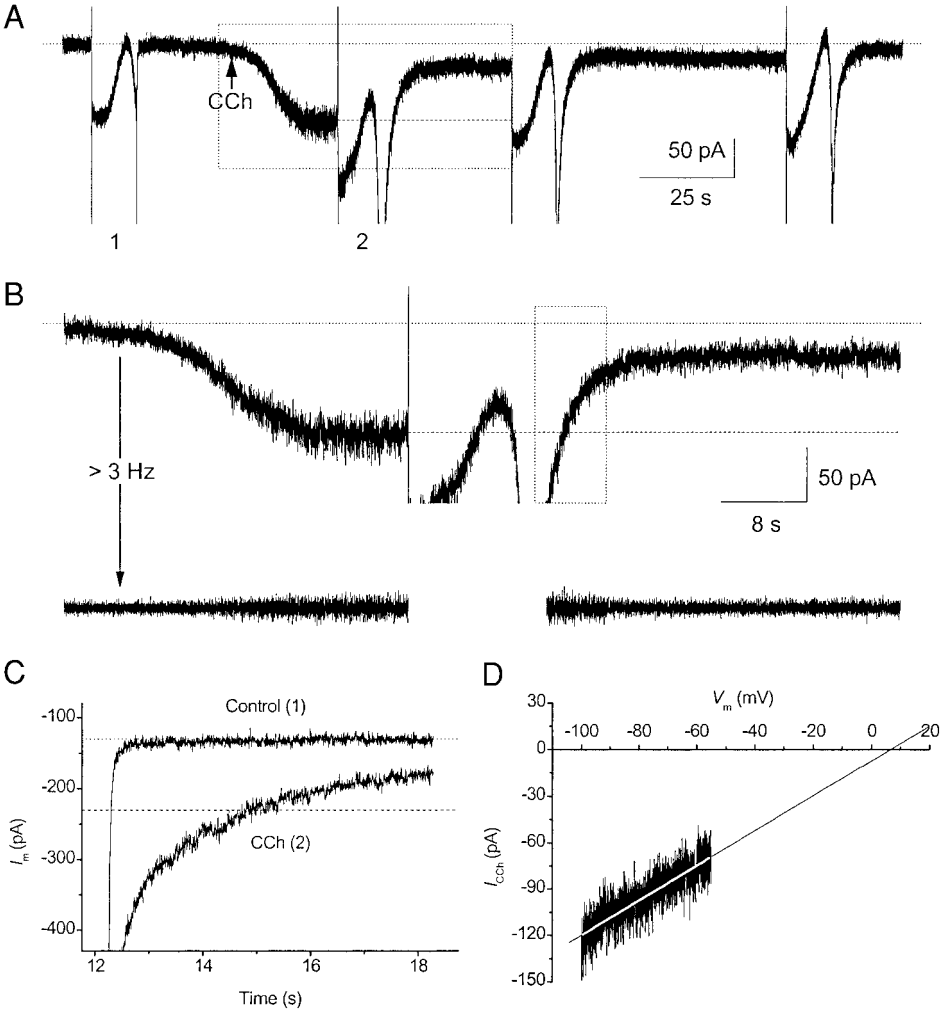

FIG. 8. Sequential postramp potentiation and downregulation of CCh-induced inward current in intracellular Cs^+. *A*: voltage-clamp recording in a representative neuron (*cell 0042601*) in the presence of 0.5 mM intrapipette EGTA (recording solutions: C_i and B_o). CCh was delivered by pressure application (8 s). Note the 4 ramp protocols applied before and during the CCh response. *B*: detail of the trace stretch delimited by the box in *A*. *Top*: the unfiltered current; *bottom*: the high-pass filtered trace (cutoff frequency: 3 Hz) which highlights the noise modifications associated with the current response. *C*: detail of the delimited postramp current (· · ·) in *B*. The postramp current in control conditions is also shown for comparison. - - -, the current level corresponding to the preramp current amplitude. *D*: the *I-V* relationship of CCh-induced currents obtained by subtraction of ramp currents. The straight line is the linear regression to data points, which returned an extrapolated reversal potential of +6.6 mV.

in a dual way. This concept will be further developed in the DISCUSSION.

DISCUSSION

The results of the present study demonstrate that in EC layer-II principal neurons the activation of muscarinic receptors causes depolarization via both the block of a K^+ conductance and, very significantly, the activation of a nonselective cation current (I_{NCM}), which displays a linear steady-state *I-V* relationship in a subthreshold range of membrane voltages (−100 to −50 mV). Importantly, taking advantage of the good signal-to-noise ratio allowed by the patch technique in our experimental conditions, we were able to implement fluctuation analysis of I_{NCM} and estimated that the cation channels underlying this current have a single-channel conductance of ~13.5 pS. Finally, we found evidence that activation of I_{NCM} per se may not require rises in intracellular Ca^{2+} concentration ($[Ca^{2+}]_i$) because the current could be induced in the presence of 10 mM EGTA or BAPTA.

Mechanisms underlying muscarinic depolarization of EC layer-II neurons and basic properties of I_{NCM}

The possibility that in EC layer-II neurons the depolarization promoted by muscarinic stimuli results from a combined action consisting in opening and closing of distinct populations of ion channels emerged from our initial current-clamp observations. These revealed that the CCh-induced depolarization includes an initial phase associated with a decrease or no detectable changes in input resistance and a later phase accompanied by an apparent increase in input resistance. The dual nature of the CCh-dependent depolarizing response was confirmed by further voltage-clamp analysis. Indeed in the absence of K^+-channel blockers CCh evoked a slowly developing inward current that at its peak displayed no apparent reversal over the entire voltage range explored (−100 to −30 mV). By contrast, during the late decay phase of the CCh-induced inward current deflection the total *I-V* plot crossed the plot obtained under control conditions in a manner entirely consistent with the block of a relatively linear K^+ conductance. In addition, we found that during extracellular application of Ba^{2+}, known to block several K^+ conductances, CCh evoked an inward current that always decreased linearly with voltage in the range from −100 to −60/−50 mV and displayed an extrapolated reversal potential at ~0 mV. This value was obtained, however, under the assumption that the slope conductance of the current under study remained constant over the voltage range of extrapolation. Our data demonstrated, nevertheless, that in EC layer-II neurons muscarinic depolarization is caused by the combined activation of a nonspecific cation current (I_{NCM}) and the slow, long-lasting block of a Ba^{2+}-sensitive K^+-conductance.

Consistently with the nonspecific nature of the cation channels underlying I_{NCM}, the reversal potential of the same current was not changed by complete substitution of intracellular K^+ with Cs^+. I_{NCM} reversal shifted in the negative direction when the extracellular Na^+ concentration was lowered, thus indicating that Na^+ is a main charge carrier for this current.

Perhaps the strongest piece of evidence that the activation of channels generating an inward current is a mechanism implied in the depolarizing effect of muscarinic stimulation in EC neurons came from our fluctuation analysis, which clearly demonstrated an increase in channel activity during the CCh-induced depolarizing current response. Noise analysis techniques have been previously satisfactorily applied to in situ central neurons for the study of the channels underlying the slow afterhyperpolarization present in hippocampal pyramidal neurons (Sah and Isaacson 1995) and dentate granule cells (Valiante et al. 1997). Our data provided an estimate for the single-channel conductance of I_{NCM} channels of ~13.5 pS. Clearly, this estimate could simply provide a lower limit for the actual value if the channels were mainly localized at electrotonically distal regions of the dendritic arbor (Valiante et al. 1997).

The activation of the here-described I_{NCM} on muscarinic stimulation appeared independent of $[Ca^{2+}]_i$ elevations because I_{NCM} responses of similar amplitude were evoked in the presence of both low and high $[Ca^{2+}]_i$ buffering capacities. Nonetheless, low intracellular levels of $[Ca^{2+}]_i$ chelators revealed prominent changes in muscarinic-receptor-dependent inward current secondarily to the application of depolarizing ramps. Prominent postramp transient, extra inward currents ("tail-like currents") were consistently observed under these conditions. In addition, in the presence of Cs^+ as the main intracellular cation, tail-like currents were followed by a marked depression of I_{NCM} amplitude and channel noise. Since ramp-triggered inward tail-like currents were abolished by high $[Ca^{2+}]_i$ buffering capacities, it seems likely that these currents were induced by transient increases in $[Ca^{2+}]_i$ due to the voltage-dependent Ca^{2+} entry elicited by the depolarization itself. Moreover, the fact that ramp depolarizations also induced a marked I_{NCM} downregulation when Cs^+ was included in the patch pipette to block K^+ conductances (which is likely to further enhance voltage-dependent Ca^{2+} influx in intact neurons) suggests that this phenomenon is also Ca^{2+}-dependent and that it may require $[Ca^{2+}]_i$ to reach higher levels than those leading to activation of extra inward currents. It appears, therefore that muscarinic-receptor-dependent induction of depolarizing current(s) may be substantially affected by Ca^{2+}-dependent modulatory processes, in the sense of both up- and downregulation. Ca^{2+}-sensitive inactivation and/or facilitation is a phenomenon well known to occur in a variety of cationic channels, including voltage-activated Ca^{2+} channels (Gutnick et al. 1989; Zuhlke et al. 1999), *N*-methyl-D-aspartate receptors (Legendre et al. 1993), cyclic nucleotide-activated cation channels (Zufall et al. 1991), and the *trp* family of channels (Hardie and Minke 1994; Ranganathan et al. 1991). Interactions between physiological processes involving positive and negative feed-back mechanisms allow physiological signals to exhibit emergent properties, most notably bistability and oscillation. It is therefore conceivable that a Ca^{2+}-dependent up- and downregulation of I_{NCM} could be at the basis of the *plateau* potentials and bursting activities that emerge in EC layer-II neurons under muscarinic modulation (Klink and Alonso 1997b,c). The bases and mechanisms of Ca^{2+}-dependent modulatory processes affecting of I_{NCM}, as well as the functional implications of such processes in firing pattern generation, are currently under study.

Possible functional correlates of I_{NCM} in the CNS

Whereas the ability of muscarinic-receptor activation to depolarize central neurons through the block of K^+ conduc-

tances is a well established observation (Benardo and Prince 1982b; Brown et al. 1997; Krnjevic 1993; Madison et al. 1987), less is known with regard to the activation of cation currents as a mechanism of muscarinic action in neurons. Muscarinic stimuli are known to cause membrane depolarization via the activation a nonspecific cation current in nonneural excitable tissues (Benham et al. 1985; Inoue et al. 1987). There is also previous evidence that in hippocampal pyramidal cells (Benson et al. 1988; Guérineau et al. 1995; Segal 1982) and interneurons (McQuiston and Madison 1999) and in *locus coeruleus* neurons (Shen and North 1992) muscarinic-receptor-dependent membrane depolarization results from both block of a K^+ conductance and activation of a cation conductance. Recently, Haj-Dahmane and Andrade (1996) have also demonstrated muscarinic activation of a nonselective cation current in rat prefrontal-cortex neurons, where muscarinic depolarization appeared to be entirely K^+-conductance independent. A major feature of the muscarinic-receptor-induced cation current in prefrontal-cortex cells was found to be a very pronounced outward rectification at potentials negative to about −40 mV, which could account for the apparent increase in input resistance that accompanies muscarinic depolarization in the same neurons. This was clearly not the case for the I_{NCM} of EC neurons described here, which, over the same voltage window, displayed a nearly ohmic behavior. This and other differences could imply that multiple, functionally different types of cation channels operated or modulated by muscarinic receptors exist in central neurons (Guérineau et al. 1995).

A striking feature of I_{NCM} was its "noisy" character. This property has not been described for muscarinic activated nonspecific cation currents in prefrontal cortex (Haj-Dahmane and Andrade 1996) or other central neurons (Guérineau et al. 1995; Shen and North 1992) and, again, this may suggests different muscarinic-receptor-activated cation currents in different brain neurons. More importantly, the association of muscarinic depolarization to the induction of membrane-current fluctuations may have important functional implications. It is well known that channel noise can deeply affect the dynamics of neurons (recently reviewed by White et al. 2000). Modeling studies have shown, for example, that in EC layer-II neurons channel noise increases excitability and enhances the resonance of these cells to periodic signals such as "theta" oscillations (White et al. 1998). Indeed, muscarinic activation facilitates the emergence of intrinsic "theta" oscillations by the EC layer-II cells as shown in vitro (Klink and Alonso 1997b) and contributes to the induction of EC "theta" rhythm in vivo (Alonso and García-Austt 1987b; Mitchell et al. 1982). Significantly, it has also been shown that additive noise can increase responsiveness, influence spike timing reliability and improve signal detection (Douglass et al. 1993; Ho and Destexhe 2000; Hunter et al. 1998; Levin and Miller 1996; Mainen and Sejnowski 1995; Tang et al. 1997a). Similarly to what has been proposed for "persistent" Na^+-channel noise in EC layer-II neurons (White et al. 1998), the membrane fluctuations caused by I_{NCM} activation might play a role, through a resonance phenomenon, in facilitating oscillatory dynamics and/or spike timing reliability, thereby influencing the learning and memory functions of EC.

Group-I metabotropic glutamate receptors (mGluR) have also been shown to cause membrane depolarization in hippocampal pyramidal cells by eliciting a nonselective cation current (Congar et al. 1997). This current was found to depend on $[Ca^{2+}]_i$ rises for its activation and therefore is probably related to the family of Ca^{2+}-activated nonselective cation currents referred to as I_{CAN} (Colquhoun et al. 1981; Partridge et al. 1994). In EC neurons, we found, however, that the development of I_{NCM} was not significantly affected by intracellular Ca^{2+} buffering with BAPTA (10 mM) thus questioning its possible relationship with I_{CAN}. A similar observation was made with respect to the nonselective cationic conductance activated by metabotropic glutamate and muscarinic agonists in CA3 pyramidal cells in organotipic slice cultures (Guérineau et al. 1995).

What molecular substrates for I_{NCM}?

As mentioned in the preceding text, in visceral smooth muscle, activation of muscarinic receptors is also known to cause membrane depolarization via the induction of a nonspecific cation current (frequently referred to as I_{CAT}) that has been thoroughly characterized (Benham et al. 1985; Inoue et al. 1987; see Kuriyama et al. 1998 for recent review). In contrast to the current described here, the amplitude of which was found to depend linearly on voltage over a wide range of membrane potentials, I_{CAT} displays a characteristic U-shaped, outward-rectifying *I-V* relationship in a negative voltage range (Inoue and Isenberg 1990a). Nevertheless, I_{CAT} also shows some clear analogies with the I_{NCM} present in EC neurons. The reported conductance of I_{CAT} channels, derived from single-channel recordings, is 20–25 pS (Benham et al. 1985; Inoue et al. 1987), a value not far from our estimation for I_{NCM} channels. I_{CAT} is Ca^{2+}-sensitive (Inoue and Isenberg 1990b; Kim et al. 1998; Pacaud and Bolton 1991), which is also the case for I_{NCM} that, although insensitive to 10 mM intracellular EGTA or BAPTA for its basal induction by muscarinic stimuli, appears to be up- and downregulated by Ca^{2+} influx. It has been suggested that I_{CAT} may belong to the *trp* family of cation channels (Walker et al. 2001; Zholos et al. 2000). Seven mammalian homologs (TRPC1–7) of the *Drosophila trp* and *trpl* genes have been identified (see Harteneck et al. 2000 for recent review) and some of them are widely expressed in brain tissue, including the cortex (Mizuno et al. 1999). Whereas some TRP channels (TRPC1, -4, -5) are mainly permeable to Ca^{2+} and activated by Ca^{2+}-store depletion (Philipp et al. 1996, 1998; Zitt et al. 1996), others, such as TRPC6, have been shown to mediate a muscarinic-receptor-activated, nonselective cation conductance (Boulay et al. 1997). Conductances resulting from the TRPC6 gene can be activated by receptors coupled to G proteins of the G_q class through signaling pathways independent of Ca^{2+}-store depletion (Boulay et al. 1997; Hofmann et al. 1999; Zhang and Saffen 2001). The following analogies between TRPC6 (and TRPC6-like gene products) and I_{NCM} channels thus emerge: both might be related to I_{CAT}; both give rise to nonselective cation currents that behave linearly over voltage (Boulay et al. 1997; Okada et al. 1999); and both are likely to depend on G proteins of the G_q class for activation because I_{NCM} is known to be activated by muscarinic re-

ceptors of the M1 subtype (Klink and Alonso 1997c) which couple to G_q (Felder 1995; Mullaney et al. 1996). While much remains to be investigated with respect to I_{NCM} channels (including their potential permeability to Ca^{2+}), the preceding elements suggest the possibility that I_{NCM} may be related to the *trp* gene family, which would open interesting perspectives on the roles of the members of this group in neuronal function (Li et al. 1999).

Concluding remarks

In the present study, we have demonstrated that an important mechanism of muscarinic depolarization in EC layer-II neurons is the activation of a "noisy" nonspecific cation current that we refer to as I_{NCM}. This current behaves linearly in the subthreshold range of membrane potentials, and the activation of I_{NCM} channels combined with the block of a K^+ conductance brings the cells toward firing threshold without necessarily causing a major change in input conductance. On the one hand, this membrane depolarization alone facilitates the expression of the intrinsic subthreshold oscillatory activity typical of most EC-layer II neurons and the generation of persistent activity (Klink and Alonso 1997b). On the other, the association of muscarinic depolarization with enhanced membrane fluctuations brought about by I_{NCM} channel noise would also facilitate oscillatory dynamics (White et al. 1998) as well as improve signal detection and firing reliability (Mainen and Sejnowski 1995; Tang et al. 1997a), thereby potentially contributing to the memory function of the EC.

We thank M. Hasselmo, E. Fransén, and C. Leonard for helpful comments on this manuscript.

This work has been supported by the Canadian Institutes of Health Research and National Institute of Mental Health Grant R01 MH-61492.

REFERENCES

ALLEN TG AND BROWN DA. M_2 muscarinic receptor-mediated inhibition of the Ca^{2+} current in rat magnocellular cholinergic basal forebrain neurones. *J Physiol (Lond)* 466: 173–189, 1993.

ALONSO A AND GARCÍA-AUSTT E. Neuronal sources of theta rhythm in the entorhinal cortex of the rat. II. Phase relations between unit discharges and theta field potentials. *Exp Brain Res* 67: 502–509, 1987a.

ALONSO A AND GARCÍA-AUSTT E. Neuronal sources of theta rhythm in the entorhinal cortex. I. Laminar distribution of theta field potentials. *Exp Brain Res* 67: 493–501, 1987b.

ALONSO A AND KLINK R. Differential electroresponsiveness of stellate and pyramidal-like cells of medial entorhinal cortex layer II. *J Neurophysiol* 70: 128–143, 1993.

ALONSO A AND KOHLER C. A study of the reciprocal connections between the septum and the entorhinal area using anterograde and retrograde axonal transport methods in the rat brain. *J Comp Neurol* 225: 327–343, 1984.

ALONSO JR AND AMARAL DG. Cholinergic innervation of the primate hippocampal formation. I. Distribution of choline acetyltransferase immunoreactivity in the *Macaca fascicularis* and *Macaca mulatta* monkeys. *J Comp Neurol* 355: 135–170, 1995.

ANDERSEN P, HOLMQVIST B, AND VOORHOEVE PE. Entorhinal activation of dentate granule cells. *Acta Physiol Scand* 66: 448–460, 1966.

ANDERSON CR AND STEVENS CF. Voltage clamp analysis of acetylcholine produced end-plate current fluctuations at frog neuromuscular junction. *J Physiol (Lond)* 235: 655–691, 1973.

BENARDO LS AND PRINCE DA. Ionic mechanisms of cholinergic excitation in mammalian hippocampal pyramidal cells. *Brain Res* 249: 333–344, 1982a.

BENARDO LS AND PRINCE DA. Cholinergic excitation of mammalian hippocampal pyramidal cells. *Brain Res* 249: 315–331, 1982b.

BENHAM CD, BOLTON TB, AND LANG RJ. Acetylcholine activates an inward current in single mammalian smooth muscle cells. *Nature* 316: 345–346, 1985.

BENSON DM, BLITZER RD, AND LANDAU EM. An analysis of the depolarization produced in guinea pig hippocampus by cholinergic receptor stimulation. *J Physiol (Lond)* 404: 479–496, 1988.

BOULAY G, ZHU X, PEYTON M, JIANG M, HURST R, STEFANI E, AND BIRNBAUMER L. Cloning and expression of a novel mammalian homolog of *Drosophila* transient receptor potential (Trp) involved in calcium entry secondary to activation of receptors coupled by the Gq class of G protein. *J Biol Chem* 272: 29672–29680, 1997.

BROWN DA, ABOGADIE FC, ALLEN TG, BUCKLEY NJ, CAULFIELD MP, DELMAS P, HALEY JE, LAMAS JA, AND SELYANKO AA. Muscarinic mechanisms in nerve cells. *Life Sci* 60: 1137–1144, 1997.

CASAMENTI F, DEFFENU G, ABBAMONDI A, AND PEPEU G. Changes in cortical acetylcholine output induced by modulation of the nucleus basalis. *Brain Res Bull* 16: 689–695, 1986.

CELESIA GG AND JASPER HH. Acetylcholine released from cerebral cortex in relation to state of activation. *Neurology* 16: 1053–1070, 1966.

CHARPAK S, GAHWLIER BH, DO KQ, AND KNOPFEL T. Potassium conductances in hippocampal neurons blocked by excitatory amino-acid transmitters. *Nature* 347: 765–767, 1990.

COLE AE AND NICOLL RA. Characterization of a slow cholinergic post-synaptic potential recorded "in vitro" from rat hippocampal pyramidal cells. *J Physiol (Lond)* 352: 173–188, 1984.

COLINO A AND HALLIWELL JV. Carbachol potentiates Q current and activates a calcium-dependent non-specific conductance in rat hippocampus in vitro. *Eur J Neurosci* 5: 1198–1209, 1993.

COLQUHOUN D, NEHER E, REUTER H, AND STEVENS CF. Inward current channels activated by intracellular Ca in cultured cardiac cells. *Nature* 294: 752–754, 1981.

CONGAR P, LEINEKUGEL X, BEN-ARI Y, AND CREPEL V. A long-lasting calcium-activated nonselective cationic current is generated by synaptic stimulation or exogenous activation of group I metabotropic glutamate receptors in CA1 pyramidal neurons. *J Neurosci* 17: 5366–5379, 1997.

DICKSON CT, MAGISTRETTI J, SHALINSKY MH, FRANSEN E, HASSELMO ME, AND ALONSO A. Properties and role of *I*(h) in the pacing of subthreshold oscillations in entorhinal cortex layer II neurons. *J Neurophysiol* 83: 2562–2579, 2000.

DOUGLASS JK, WILKENS L, PANTAZELOU E, AND MOSS F. Noise enhancement of information transfer in crayfish mechanoreceptors by stochastic resonance. *Nature* 365: 337–340, 1993.

DYKES RW. Mechanisms controlling neuronal plasticity in somatosensory cortex. *Can J Physiol Pharmacol* 75: 535–545, 1997.

EGAN TM AND NORTH RA. Acetylcholine acts on m_2-muscarinic receptors to excite rat locus coeruleus neurons. *Br J Pharmacol* 85: 733–735, 1985.

FELDER CC. Muscarinic acetylcholine receptors: signal transduction through multiple effectors. *Faseb J* 9: 619–625, 1995.

GUÉRINEAU NC, BOSSU J-L, GÄHWILER BH, AND GERBERG U. Activation of a non-selective cationic conductance by metabotropic glutamatergic and muscarinic agonists in CA3 pyramidal neurons of the rat hippocampus. *J Neurosci* 15: 4435–4407, 1995.

GUTNICK MJ, LUX HD, SWANDULLA D, AND ZUCKER H. Voltage-dependent and calcium-dependent inactivation of calcium channel current in identified snail neurones. *J Physiol (Lond)* 412: 197–220, 1989.

HAJ-DAHMANE S AND ANDRADE R. Muscarinic activation of a voltage-dependent cation non-selective current in rat association cortex. *J Neurosci* 16: 3848–3861, 1996.

HAJ-DAHMANE S AND ANDRADE R. Ionic mechanism of the slow afterdepolarization induced by muscarinic receptor activation in rat prefrontal cortex. *J Neurophysiol* 80: 1197–1210, 1998.

HALLIWELL JV AND ADAMS PR. Voltage-clamp analysis of muscarinic excitation in hippocampal neurons. *Brain Res* 250: 71–92, 1982.

HAMILL OP, MARTY A, NEHER E, SAKMANN B, AND SIGWORTH FJ. Improved patch-clamp techniques for high-resolution current recording from cells and cell-free membrane patches. *Pflügers Arch* 391: 85–100, 1981.

HARDIE RC AND MINKE B. Calcium-dependent inactivation of light-sensitive channels in *Drosophila* photoreceptors. *J Gen Physiol* 103: 409–427, 1994.

HARTENECK C, PLANT TD, AND SCHULTZ G. From worm to man: three subfamilies of TRP channels. *Trends Neurosci* 23: 159–166, 2000.

HARVEY J, BALASUBRAMANIAM R, AND COLLINGRIDGE GL. Carbachol can potentiate *N*-methyl-D-aspartate responses in the rat hippocampus by a staurosporine and thapsigargin-insensitive mechanism. *Neurosci Lett* 162: 165–168, 1993.

HASSELMO ME AND BOWER JM. Acetylcholine and memory. *Trends Neurosci* 16: 218–222, 1993.

HASSELMO ME AND SCHNELL E. Laminar selectivity of the cholinergic suppression of synaptic transmission in rat hippocampal region CA1: computational modeling and brain slice physiology. *J Neurosci* 14: 3898–3914, 1994.

HIGASHIDA H, HASHII M, FUKUDA K, CAULFIELD MP, NUMA S, AND BROWN DA. Selective coupling of different muscarinic acetylcholine receptors to neuronal calcium currents in DNA-transfected cells. *Proc R Soc Lond B Biol Sci* 242: 68–74, 1990.

HILLE B. *Ionic Channels of Excitable Membranes.* Sunderland, MA: Sinauer, 1992.

HO N AND DESTEXHE A. Synaptic background activity enhances the responsiveness of neocortical pyramidal neurons. *J Neurophysiol* 84: 1488–1496, 2000.

HOFMANN T, OBUKHOV AG, SCHAEFER M, HARTENECK C, GUDERMANN T, AND SCHULTZ G. Direct activation of human TRPC6 and TRPC3 channels by diacylglycerol. *Nature* 397: 259–263, 1999.

HUNTER JD, MILTON JG, THOMAS PJ, AND COWAN JD. Resonance effect for neural spike time reliability. *J Neurophysiol* 80: 1427–1438, 1998.

INOUE R AND ISENBERG G. Effect of membrane potential on acethylcholine-induced inward current in guinea pig ileum. *J Physiol (Lond)* 424: 57–71, 1990a.

INOUE R AND ISENBERG G. Intracellular calcium ions modulate acetylcholine-induced inward current in guinea pig ileum. *J Physiol (Lond)* 424: 73–92, 1990b.

INOUE R, KITAMURA K, AND KURIYAMA H. Acetylcholine activates single sodium channels in smooth muscle cells. *Pflügers Arch* 410: 69–74, 1987.

KIM YC, KIM SJ, SIM JH, JUN JY, KANG TM, SUH SH, SO I, AND KIM KW. Protein kinase C mediates the desensitization of CCh-activated nonselective cationic current in guinea pig gastric myocytes. *Pflügers Arch* 436: 1–8, 1998.

KLINK R AND ALONSO A. Morphological characteristics of layer II projection neurons in the rat medial entorhinal cortex. *Hippocampus* 7: 571–583, 1997a.

KLINK R AND ALONSO A. Muscarinic modulation of the oscillatory and repetitive firing properties of entorhinal cortex layer II neurons. *J Neurophysiol* 77: 1813–1828, 1997b.

KLINK R AND ALONSO A. Ionic mechanisms of muscarinic depolarization in entorhinal cortex layer II neurons. *J Neurophysiol* 77: 1829–1843, 1997c.

KRNJEVIC K. Central cholinergic mechanisms and function. *Prog Brain Res* 1993: 285–292, 1993.

KURIYAMA H, KITAMURA K, ITOH T, AND INOUE R. Physiological features of visceral smooth muscle cells, with special reference to receptors and ion channels. *Physiol Rev* 78: 811–920, 1998.

LEGENDRE P, ROSENMUND C, AND WESTBROOK GL. Inactivation of NMDA channels in cultured hippocampal neurons by intracellular calcium. *J Neurosci* 13: 674–684, 1993.

LEVIN JE AND MILLER JP. Broadband neural encoding in the cricket cercal sensory system enhanced by stochastic resonance. *Nature* 380: 165–168, 1996.

LI HS, XU XZ, AND MONTELL C. Activation of a TRPC3-dependent cation current through the neurotrophin BDNF. *Neuron* 24: 261–273, 1999.

MADISON DV, LANCASTER B, AND NICOLL RA. Voltage-clamp analysis of cholinergic action in the hippocampus. *J Neurosci* 7: 733–741, 1987.

MAGISTRETTI J, AND ALONSO A. Biophysical properties and slow voltage-dependent inactivation of a sustained sodium current in entorhinal cortex layer-II principal neurons. A whole cell and single-channel study. *J Gen Physiol* 114: 491–509, 1999.

MAINEN ZF AND SEJNOWSKI TJ. Reliability of spike timing in neocortical neurons. *Science* 268: 1503–1506, 1995.

MARINO MJ, ROUSE ST, LEVEY AI, POTTER LT, AND CONN PJ. Activation of the genetically defined m1 muscarinic receptor potentiates *N*-methyl-D-aspartate (NMDA) receptor currents in hippocampal pyramidal cells. *Proc Natl Acad Sci USA* 95: 11465–11470, 1998.

MARKRAM H AND SEGAL M. The inositol 1,4,5-trisphosphate pathway mediates cholinergic potentiation of rat hippocampal neuronal responses to NMDA. *J Physiol (Lond)* 447: 513–533, 1992.

MATHIE A, BERNHEIM L, AND HILLE B. Inhibition of N- and L-type calcium channels by muscarinic receptor activation in rat sympathetic neurons. *Neuron* 8: 907–914, 1992.

MCCORMICK DA AND PRINCE DA. Mechanisms of action of acetylcholine in the guinea pig cerebral cortex in vitro. *J Physiol (Lond)* 375: 169–194, 1986.

MCQUISTON AR AND MADISON DV. Muscarinic receptor activity has multiple effects on the resting membrane potentials of CA1 hippocampal interneurons. *J Neurosci* 19: 5693–5702, 1999.

MITCHELL SJ, RAWLINS JNP, STEWARD O, AND OLTON DS. Medial septal area lesions disrupt theta rhythm and cholinergic staining in medial entorhinal cortex and produce impaired radial arm maze behavior in rats. *J Neurosci* 2: 292–302, 1982.

MIZUNO N, KITAYAMA S, SAISHIN Y, SHIMADA S, MORITA K, MITSUHATA C, KURIHARA H, AND DOHI T. Molecular cloning and characterization of rat trp homologues from brain. *Brain Res Mol Brain Res* 64: 41–51, 1999.

MULLANEY I, CAULFIELD MP, SVOBODA P, AND MILLIGAN G. Activation, cellular redistribution and enhanced degradation of the G proteins Gq and G11 by endogenously expressed and transfected phospholipase C-coupled muscarinic m1 acetylcholine receptors. *Prog Brain Res* 109: 181–187, 1996.

OKADA T, INOUE R, YAMAZAKI K, MAEDA A, KUROSAKI T, YAMAKUNI T, TANAKA I, SHIMIZU S, IKENAKA K, IMOTO K, AND MORI Y. Molecular and functional characterization of a novel mouse transient receptor potential protein homologue TRP7. Ca(2+)-permeable cation channel that is constitutively activated and enhanced by stimulation of G-protein-coupled receptor. *J Biol Chem* 274: 27359–27370, 1999.

PACAUD P AND BOLTON TB. Relation between muscarinic receptor cationic current and internal calcium in guinea pig jejunal smooth muscle cells. *J Physiol (Lond)* 441: 477–499, 1991.

PARTRIDGE LD, MULLER TH, AND SWANDULLA D. Calcium-activated nonselective channels in the nervous system. *Brain Res Rew* 19: 319–325, 1994.

PHILIPP S, CAVALIE A, FREICHEL M, WISSENBACH U, ZIMMER S, TROST C, MARQUART A, MURAKAMI M, AND FLOCKERZI V. A mammalian capacitative calcium entry channel homologous to Drosophila TRP and TRPL. *EMBO J* 15: 6166–6171, 1996.

PHILIPP S, HAMBRECHT J, BRASLAVSKI L, SCHROTH G, FREICHEL M, MURAKAMI M, CAVALIE A, AND FLOCKERZI V. A novel capacitative calcium entry channel expressed in excitable cells. *EMBO J* 17: 4274–4282, 1998.

RANGANATHAN R, HARRIS GL, STEVENS CF, AND ZUKER CS. A *Drosophila* mutant defective in extracellular calcium-dependent photoreceptor deactivation and rapid desensitization. *Nature* 354: 230–232, 1991.

RICHARDSON RT AND DELONG MR. A reappraisal of the functions of the nucleus basalis of Meynert. *Trends Neurosci* 11: 264–267, 1988.

SAH P AND ISAACSON JS. Channels underlying the slow afterhyperpolarization in hippocampal pyramidal neurons: neurotransmitters modulate the open probability. *Neuron* 15: 435–441, 1995.

SCHWARTZ SP AND COLEMAN PD. Neurons of origin of the perforant path. *Exp Neurol* 74: 305–312, 1981.

SCOVILLE WB AND MILNER B. Loss of recent memory after bilateral hippocampal lesions. *J Neurol Neurosurg Psychiatry* 20: 11–21, 1957.

SEGAL M. Multiple actions of acetylcholine at a muscarinic receptor studied in the rat hippocampal slice. *Brain Res* 246: 77–87, 1982.

SHEN K-Z AND NORTH RA. Muscarine increases cation conductance and decreases potassium conductance in rat locus coeruleus neurons. *J Physiol (Lond)* 455: 471–485, 1992.

SHULZ DE, SOSNIK R, EGO V, HAIDARLIU S, AND AHISSAR E. A neuronal analogue of state-dependent learning. *Nature* 403: 549–553, 2000.

SIGWORTH FJ. The variance of sodium current fluctuations at the node of Ranvier. *J Physiol (Lond)* 307: 97–129, 1980.

SQUIRE LR. Memory systems. *C R Acad Sci III* 321: 153–156, 1998.

TANG AC, BARTELS AM, AND SEJNOWSKI TJ. Effects of cholinergic modulation on responses of neocortical neurons to fluctuating input. *Cereb Cortex* 7: 502–509, 1997.

TANG Y, MISHKIN M, AND AIGNER TG. Effects of muscarinic blockade in perirhinal cortex during visual recognition. *Proc Natl Acad Sci USA* 94: 12667–12669, 1997.

TOSELLI M AND TAGLIETTI V. Muscarine inhibits high-threshold calcium currents with two distinct modes in rat embryonic hippocampal neurons. *J Physiol (Lond)* 483: 347–365, 1995.

TSUBOKAWA H AND ROSS WN. Muscarinic modulation of spike backpropagation in the apical dendrites of hippocampal CA1 pyramidal neurons. *J Neurosci* 17: 5782–5791, 1997.

VALIANTE TA, ABDUL-GHANI MA, CARLEN PL, AND PENNEFATHER P. Analysis of current fluctuations during after-hyperpolarization current in dentate granule neurones of the rat hippocampus. *J Physiol (Lond)* 499: 121–134, 1997.

WALKER RL, HUME JR, AND HOROWITZ B. Differential expression and alternate splicing of TRP channel genes in smooth muscles. *Am J Physiol Cell Physiol* 280: C1184–C1192, 2001.

WANKE E, BIANCHI L, MANTEGAZZA M, GUATTEO E, MANCINELLI E, AND FERRONI A. Muscarinic regulation of Ca^{2+} currents in rat sensory neurons: channel and receptor types, dose-response relationships and cross-talk pathways. *Eur J Neurosci* 6: 381–391, 1994.

WANKE E, FERRONI A, MALGAROLI A, AMBROSINI A, POZZAN T, AND MELDOLESI J. Activation of a muscarinic receptor selectively inhibits a rapidly inactivated Ca^{2+} current in rat sympathetic neurons. *Proc Natl Acad Sci USA* 84: 4313–4317, 1987.

WHITE JA, KLINK R, ALONSO A, AND KAY AR. Noise from voltage-gated ion channels may influence neuronal dynamics in the entorhinal cortex. *J Neurophysiol* 80: 262–269, 1998.

WHITE JA, RUBINSTEIN JT, AND KAY AR. Channel noise in neurons. *Trends Neurosci* 23: 131–137, 2000.

ZHANG L AND SAFFEN D. Muscarinic acetylcholine receptor regulation of TRP6 Ca^{2+} channel isoforms: molecular structures and functional characterization. *J Biol Chem* 276: 13331–13339, 2001.

ZHOLOS AV, TSYTSYURA YD, PHILYPPOV IB, SHUBA MF, AND BOLTON TB. Voltage-dependent inhibition of the muscarinic cationic current in guinea pig ileal cells by SK and F 96365. *Br J Pharmacol* 129: 695–702, 2000.

ZITT C, ZOBEL A, OBUKHOV AG, HARTENECK C, KALKBRENER F, LUCKHOFF A, AND SCHULTZ G. Cloning and functional expression of a human Ca^{2+}-permeable cation channel activated by calcium store depletion. *Neuron* 16: 1189–1196, 1996.

ZUFALL F, SHEPHERD GM, AND FIRESTEIN S. Inhibition of the olfactory cyclic nucleotide gated ion channel by intracellular calcium. *Proc R Soc Lond B Biol Sci* 246: 225–230, 1991.

ZUHLKE RD, PITT GS, DEISSEROTH K, TSIEN RW, AND REUTER H. Calmodulin supports both inactivation and facilitation of L-type calcium channels. *Nature* 399: 159–162, 1999.